

# Text2Structure3D: Graph-Based Generative Modeling of Equilibrium Structures with Diffusion Transformers

Lazlo Bleker<sup>a,b,\*</sup>, Zifeng Guo<sup>c</sup>, Kaleb Smith<sup>d</sup>, Kam-Ming Mark Tam<sup>e</sup>, Karla Saldaña Ochoa<sup>f</sup>, Pierluigi D’Acunto<sup>a,b,g</sup>

<sup>a</sup>Technical University of Munich, School of Engineering and Design, Professorship of Structural Design, Arcisstraße 21, Munich, 80333, Germany

<sup>b</sup>Technical University of Munich, Munich Data Science Institute, Walther-von-Dyck-Straße 10, Garching, 85748, Germany

<sup>c</sup>Strabag AG, Albstadtweg 3, Stuttgart, 70567, Germany

<sup>d</sup>NVIDIA, Gainesville, USA

<sup>e</sup>University of Hong Kong, Department of Architecture, 4/F, Knowles Building, Pokfulam Road, Hong Kong SAR, China

<sup>f</sup>University of Florida, School of Architecture, College of Design, Construction and Planning, Gainesville, USA

<sup>g</sup>Technical University of Munich, Institute for Advanced Study, Lichtenbergstraße 2a, Garching, 85748, Germany

## Abstract

This paper presents Text2Structure3D, a graph-based Machine Learning (ML) model that generates equilibrium structures from natural language prompts. Text2Structure3D is designed to support new intuitive ways of design exploration and iteration in the conceptual structural design process. The approach combines latent diffusion with a Variational Graph Auto-Encoder (VGAЕ) and graph transformers to generate structural graphs that are close to an equilibrium state. Text2Structure3D integrates a residual force optimization post-processing step that ensures generated structures fully satisfy static equilibrium. The model was trained and validated using a cross-typological dataset of funicular form-found and statically determinate bridge structures, paired with text descriptions that capture the formal and structural features of each bridge. Results demonstrate that Text2Structure3D generates equilibrium structures with strong adherence to text-based specifications and greatly improves generalization capabilities compared to parametric model-based approaches. Text2Structure3D represents an early step toward a general-purpose foundation model for structural design, enabling the integration of generative AI into conceptual design workflows.

**Keywords:** Machine Learning, Graph Machine Learning, Diffusion, Structural Design, Structural Form-Finding

## 1. Introduction

Load-bearing structures have one of the largest contributions to the total embodied carbon of buildings and infrastructure [1], highlighting the importance of efficient structural designs. A major reason for structural design inefficiencies is that structural engineers are typically only first involved in more advanced stages of design, while the impact of design decisions is largest in the preceding conceptual design phases [2]. In this regard, developments aimed at the conceptual structural design phase can potentially have an outsized impact on the sustainability of the Architecture, Engineering and Construction (AEC) industry as a whole.

Generative Artificial Intelligence (GenAI) presents a unique opportunity for enhancing the conceptual structural design process and is rapidly transforming a range of other design domains, most prominently those dealing with images, video and natural language, but also areas such as 3D modeling and molecular design. Within the AEC industry, GenAI is already being applied for general architectural design [3], automated floor plan generation [4] and generative Building Information Modeling (BIM) [5]. While there are also generative AI applications for structural design, they are generally focused

on specific tasks, limiting their rate of adoption in structural design practice.

In this regard, general-purpose generative AI for structural design—especially those accessible through intuitive inputs such as text prompts—can enable a wider exploration of efficient structural designs already in the conceptual design phase.

### 1.1. Problem Statement

Current generative AI approaches for structural design are often narrow in scope and typically confined to data representations dependent on problem-specific parametric models. This makes such approaches time-intensive to adapt to new applications, requiring the retraining of models, creation of new datasets, or even adapting the model architecture. General-purpose foundation models on the other hand represent a new paradigm in Machine Learning (ML) that aims to address these challenges by training a single model on large amounts of data that is flexible enough to adapt to a broad range of tasks. However, existing foundation models like Large Language Models (LLM) are ill-suited for structural design applications for two main reasons: (i) most operate on text and image modalities which are inefficient as structural design representations compared to more flexible data structures like graphs. and (ii) they lack domain-specific knowledge, such as spatial understanding or constraints from statics like equilibrium. This leaves open the challenge

\*Corresponding Author

Email address: [lazlo.bleker@tum.de](mailto:lazlo.bleker@tum.de) (Lazlo Bleker)

of developing generative methods that are both broadly applicable within structural design and aware of relevant physical constraints.

### 1.2. Objectives and Scope

To address the challenges of applying generative AI in structural design we present *Text2Structure3D*, a generative latent diffusion model [6] for equilibrium structures conditioned on natural language. *Text2Structure3D* operates on general graph-based data representations of discrete pin-jointed structures in line with the level of abstraction common in the conceptual design phase (Figure 1). We specifically focus on generating structures that satisfy equilibrium, being the most fundamental structural design constraint. Moreover, we condition the model on text embeddings to allow for the generation of equilibrium structures that can satisfy a variety of user-defined specifications.

### 1.3. Contributions

This study contributes to the field in the following three ways:

1. By conditioning our model on text embeddings, *Text2Structure3D* enables new and intuitive natural language-based conceptual structural design processes. Structures adhering to a wide variety of design specifications can be generated, including text descriptions containing both qualitative and quantitative attributes,
2. We introduce a graph-based model architecture (*Text2Structure3D*) consisting of latent diffusion [6], a Variational Graph Auto-Encoder (VGAE) [7], and graph transformers [8], that can generate forms and forces of structures in static equilibrium. The combination of a VGAE with diffusion enables the generation of structures from a variable-sized and connected graph space that could not be generated with a VGAE alone.
3. We jointly encode (continuous) edge force densities, (continuous) node coordinates and (categorical) support conditions into a shared node-level latent space that simplifies the latent diffusion process. The static equilibrium of reconstructions from this latent space are ensured by a residual force optimization post-processing step that combines the accuracy of geometry-based reconstructions with the physical validity of force-based reconstructions.

We train and validate *Text2Structure3D* on a cross-typological synthetic dataset of combinations of bridge structures and text descriptions. Together, *Text2Structure3D* represents a first step towards a general-purpose foundation model for the design of equilibrium structures.

## 2. Related Work

### 2.1. Generative Structural Design

The term generative design has been used in architectural and structural design since well before the most recent generative

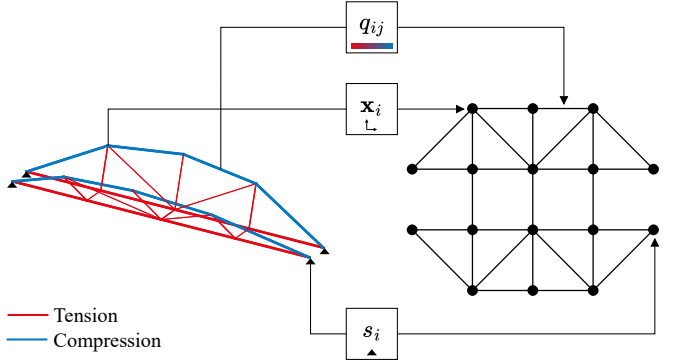


Figure 1: An equilibrium structure (left) represented as a graph (right). Every node  $i$  of the graph is embedded with the coordinates ( $\mathbf{x}_i$ ) and support condition ( $s_i$ ) of the corresponding node in the equilibrium structure. Every edge  $(i, j)$  of the graph contains the force density ( $q_{ij}$ ) of the corresponding member in the equilibrium structure.

AI revolution [9, 10]. These early generative design approaches are often based on parametric models [11] or structural grammars [12], encoding the structure as a (top-down) vector of design parameters, or a (bottom-up) sequence of design actions respectively. Generative design typically involves the creation of designs that satisfy certain criteria or optimize a given objective. In this regard also form-finding [13], topology optimization [14], and layout optimization [15], can be considered as forms of generative design. To satisfy design objectives, design spaces created with parametric models are commonly explored using metaheuristics such as evolutionary algorithms [16, 17].

More recently, generative AI approaches have been proposed as a powerful alternative for design space exploration. Building on previous work for performance-based design exploration [18], Danhaive and Mueller were one of the first to apply generative AI in structural design by training a Variational Auto-Encoder (VAE) [19] to encode structural designs into a latent space [20]. Bucher et al. extend on this idea by conditioning the VAE on explicit performance parameters [21], and Balmer et al. additionally include Explainable AI (XAI) methods [22, 23]. Saldana Ochoa et al. propose a structural form-finding-based generative design workflow using a discriminative ML model [24], and Guo et al. build on this approach with a Generative Adversarial Network (GAN) [25] conditioned on single word text embeddings [26]. Common to all these approaches is that they are based on parametric models that encode structural designs as vectors of model-specific design spaces. New tasks involving parametric models other than the one for which the ML model was designed will produce incompatible vector data. This presents a critical scalability limitation for parametric model-based approaches, invariably requiring retraining the model and adjusting its architecture for each new design task.

Moving beyond this limitation of vector data requires encoding structures with a more general data structure. One alternative

to parametric model-based approaches is to represent structures with higher rank tensors, such as images, instead. Examples of structural design applications using generative ML models for image data include optimal shear wall layout [27], and shell structure design [28]. Yet, image-based approach rely still rely on a fixed parameterization scheme that does not accommodate design spaces involving systems of variable sizes and connectivities. Consequently, they are ill-suited for modeling trans-topological design spaces. Naive strategies that employ image-based methods for such systems often rely on fixed sampling techniques, which lack expressivity, lead to data loss, and are unable to provide fine-grained predictions at each element, as the sampling rate does not align neatly with the system’s elements. These limitations of Euclidean tensor-based data structures motivate the exploration of alternative more general structural design representations.

## 2.2. Graph Machine Learning for Structural Design

Unlike vectors or images, graphs represent a natural way of encoding discrete structures, especially those consisting of truss or beam elements which are ubiquitous in conceptual structural design [29]. At the same time, Graph Neural Networks (GNN) [7] allow ML models to make predictions on graphs, which has been explored for a number of graph-based structural design applications. Chang and Cheng use GNNs to accelerate cross-section optimization [30], and Whalen and Mueller train a GNN as a surrogate model for truss Finite Element Method (FEM) [31]. Hayashi et al. combine GNNs with Reinforcement Learning (RL) for cross-section [32] and assembly sequence optimization [33], and Zhao et al. use GNNs for automated shear wall layout design [34]. Bleker et al. apply GNNs to structural form-finding using the Combinatorial Equilibrium Modeling (CEM) [35], first with a discriminative model [36] and later extend it with a generative model [37].

Graph-based models also naturally allow for integration with knowledge and constraints from statics and geometry. Tam et al. introduce a residual force loss that pushes predictions to equilibrium states [38, 39] and Bleker et al. apply an Equivariant Graph Neural Network (EGNN) [40] to ensure predictions are equivariant to Euclidean transformations [41].

Despite the powerful representation provided by graphs, generative models in structural design have up until now been more commonly based on tensor representations, such as vectors and images. Liao et al. give the high level of complexity and sophistication of generative graph models as one of the reasons [42]. However, recent developments in generative models for graphs have the potential of making graph models more suitable for generative structural design applications.

## 2.3. Diffusion Models

Diffusion models are a type of generative AI based on a gradual denoising process to obtain samples from a data distribution [43, 44, 45]. Stemming from computer vision, diffusion models have been popularized by applications such as DALL-E 2 by OpenAI [46] and the open-source Stable Diffusion [6], and

have since then been extended to other modalities, such as audio [47], text [48], and, most relevant to this work, graphs [49]. The most prominent domains of graph diffusion are for molecular generation, such as material and drug design, where they have become the state of the art [50, 51]. A common approach is to apply diffusion at the node-level feature space of graphs. However, this presents the challenge that features often consist of a mix of continuous and discrete variables, requiring a sophisticated and complex diffusion process [52]. To overcome this limitation, Xu et al. propose applying latent diffusion on graphs by encoding node features into a node-level latent space [53]. In this way, diffusion on a complex categorical-continuous product manifold is avoided in favor of a purely continuous latent space. This approach simplifies the modeling process and at the same time allows graphs of various types to be modeled by a single model [54].

Similar to molecular data, graph-based structural data also consists of both continuous node features (coordinates) as well as categorical features (support conditions). Moreover, unlike for molecules in which edge features can be modeled implicitly, structural data requires explicitly defined edge features, such as forces or force densities. In this work, we apply latent diffusion to graph-based equilibrium structures, encoding both categorical and continuous features, as well as node and edge features into one combined node-level latent space.

## 3. Latent Diffusion for Equilibrium Structures

Text2Structure3D is a graph-based latent diffusion model that can generate equilibrium structures from text prompts (Figure 2). During inference, a conditioning vector ( $\mathbf{c}$ ) is created by a pre-trained text embedding model. A Diffusion Transformer (DiT) conditioned on  $\mathbf{c}$  then generates a point in the latent space ( $\mathbf{z}$ ), which is decoded into a structural geometry and set of force densities ( $\hat{\mathbf{q}}$ ) by a VGAE decoder. Both the DiT and VGAE receive an additional topology input produced by a Multilayer Perceptron (MLP) conditioned on  $\mathbf{c}$  in a parallel stream. Finally, a residual force optimization post-processes the geometry and force densities ( $\hat{\mathbf{q}}$ ) to obtain the final equilibrium structure.

The individual models of Text2Structure3D are trained in a reverse order relative to the order used during inference. First, we train the VGAE to encode equilibrium structures into a latent space (Section 3.1), and to be able to reconstruct these with the help of residual force optimization to preserve equilibrium (Section 3.2). Then, we freeze the VGAE weights and use its encoder by training the DiT to generate samples from the distribution of the VGAE latent space (Section 3.3). In Section 3.4 we outline the topology MLP and finally in Section 3.5 we explain the creation of the synthetic dataset on which we train Text2Structure3D.

### 3.1. Variational Graph Auto-Encoder

The first step of Text2Structure3D involves training a Variational Graph Auto-Encoder (VGAE) [7] to encode equilibrium

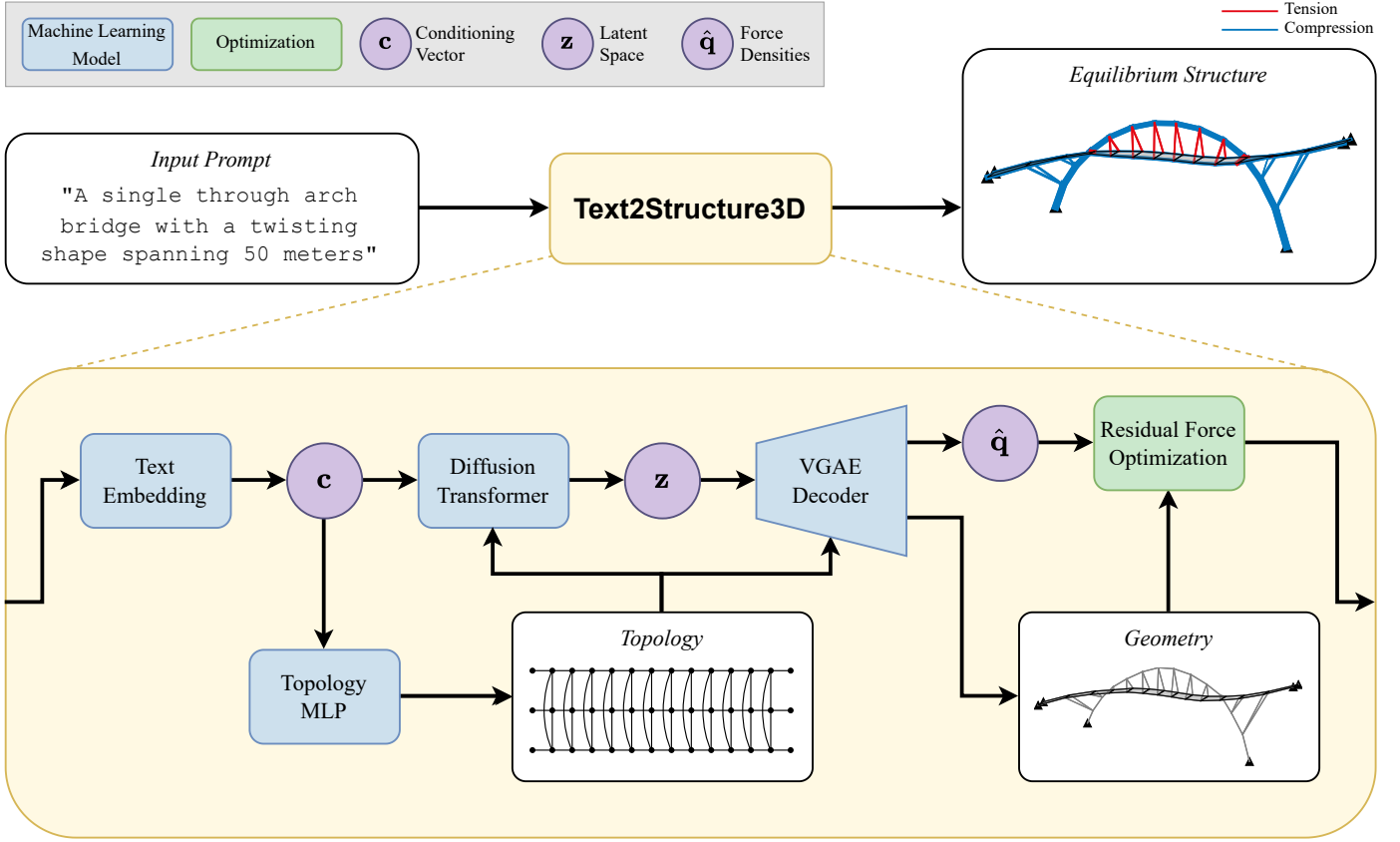


Figure 2: Text2Structure3D can generate an equilibrium structure adhering to an input text prompt. A text embedding model creates a conditioning vector ( $\mathbf{c}$ ) that is input to a diffusion transformer and a topology Multilayer Perceptron (MLP). The diffusion transformer denoises a sample in the latent space ( $\mathbf{z}$ ), conditioned on  $\mathbf{c}$  and a topology generated by the topology MLP. A VGAE Decoder [7], also conditioned by the topology, creates a geometry and set of force densities ( $\hat{\mathbf{q}}$ ) from the latent. The geometry and  $\hat{\mathbf{q}}$  are optimized together to obtain a final sample of a structure in equilibrium.

structures into a latent space. Equilibrium structures are modeled as graphs with a mix of node- and edge-level, as well as continuous and categorical features:

$$\begin{aligned}
 \text{Force density} \quad \mathbf{q} &= \{q_{ij} \mid (i, j) \in \mathcal{E}\} & \in \mathbb{R}^E, \\
 \text{Coordinates} \quad \mathbf{x} &= \{\mathbf{x}_i \mid i = 1, \dots, N\} & \in \mathbb{R}^{N \times 3}, \quad (1) \\
 \text{Support condition} \quad \mathbf{s} &= \{s_i \mid i = 1, \dots, N\} & \in \mathbb{Z}^N.
 \end{aligned}$$

Here,  $N$  is the number of nodes and  $\mathcal{E}$  the set of edges ( $|\mathcal{E}| = E$ ) that defines the structure's topology. Each edge  $(i, j) \in \mathcal{E}$  is assigned a force density  $q_{ij}$  (kN/m), while each node  $i$  is associated with coordinates  $\mathbf{x}_i$  (m) and a categorical support condition  $s_i \in \{0, 1\}$ , where 0 denotes a node as free and 1 as fixed. Here, the force density of an edge is defined as the axial force in the corresponding member ( $f_{ij}$ ) divided by its length ( $l_{ij}$ ):

$$q_{ij} = \frac{f_{ij}}{l_{ij}} \quad (2)$$

We use the edge force density for its linear relation with  $\mathbf{x}$  [55], though an edge force definition results in an equivalent representation and could also be used. It should be noted we do not explicitly model the external load, and instead derive it from

the geometry based on assumptions of the training dataset (see Section 3.5).

The VGAE encoder takes these multi-modal features as inputs and maps them into a shared node-level latent space  $\mathbf{z} \in \mathbb{R}^{N \times d_z}$ , see Figure 3. The decoder then takes  $\mathbf{z}$  and jointly reconstructs the features  $\{\hat{\mathbf{q}}, \hat{\mathbf{x}}, \hat{\mathbf{s}}\}$ .

We train the VGAE with a reconstruction loss, using a Mean Squared Error (MSE) for  $\hat{\mathbf{q}}$  and  $\hat{\mathbf{x}}$ , and a Binary Cross Entropy (BCE) for  $\hat{\mathbf{s}}$ :

$$\mathcal{L}_q = \frac{1}{E} \sum_{(i,j) \in \mathcal{E}} (\hat{q}_{ij} - q_{ij})^2, \quad (3)$$

$$\mathcal{L}_x = \frac{1}{N} \sum_{i=1}^N \|\hat{\mathbf{x}}_i - \mathbf{x}_i\|_2^2, \quad (4)$$

$$\begin{aligned}
 \mathcal{L}_s = \frac{1}{N} \sum_{i=1}^N & \left( -s_i \log \sigma(\hat{s}_i) \right. \\
 & \left. - (1 - s_i) \log(1 - \sigma(\hat{s}_i)) \right). \quad (5)
 \end{aligned}$$

Furthermore, we apply a KL divergence loss to regularize the

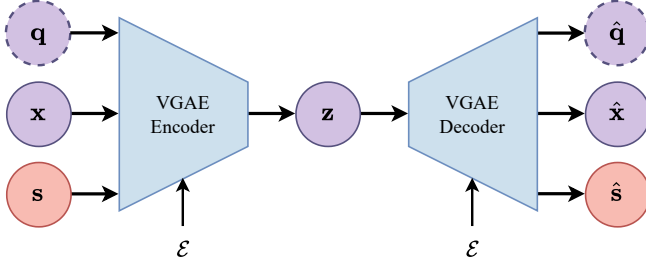


Figure 3: A Variational Graph Auto-Encoder (VGAE) [7] learns a node-level latent space by jointly reconstructing both node-level and edge-level, as well as continuous and categorical features. The features of our equilibrium data consist of the edge force density ( $\mathbf{q}$ ), the node coordinates ( $\mathbf{x}$ ) and the node support condition ( $\mathbf{s}$ ).

latent space according to

$$\mathcal{L}_{\text{KL}} = D_{\text{KL}}(\mathcal{N}(\mu_z, \sigma_z) \parallel \mathcal{N}(0, I)). \quad (6)$$

The total loss is then described as the following weighted sum:

$$\mathcal{L} = \lambda_q \mathcal{L}_q + \lambda_x \mathcal{L}_x + \lambda_s \mathcal{L}_s + \beta \mathcal{L}_{\text{KL}}. \quad (7)$$

Because we will model the latent space distribution with a diffusion model, we will not need to directly sample from the VGAE latent space and can afford a significant divergence from the Gaussian prior. Thus, we rather prioritize obtaining accurate reconstructions by setting the KL divergence weight to a low value. We found  $\beta = 0.01$  to produce good results, combined with  $\lambda_q = \lambda_x = \lambda_s = 1.0$ . For the architecture of both the encoder and decoder we use a graph transformer to the design of Rampasek et al. [56]. For additional hyperparameter details we refer to Appendix A.

### 3.2. Equilibrium-based Reconstruction

The reconstructed force densities  $\hat{\mathbf{q}}$  will in general not perfectly match the ground truth  $\mathbf{q}$ , and similarly,  $\hat{\mathbf{x}}$  will not equal  $\mathbf{x}$ . While a limited reconstruction error in both  $\hat{\mathbf{q}}$  and  $\hat{\mathbf{x}}$  is admissible, uncoordinated errors will lead to structures that are not in equilibrium. To determine if a structure is in equilibrium we can calculate its residual force according to

$$\mathbf{r}_i = \mathbf{p}_i + \sum_{j \in \mathcal{N}(i)} q_{ij} (\mathbf{x}_j - \mathbf{x}_i) \quad (8)$$

where  $\mathbf{r}_i$  and  $\mathbf{p}_i$  are the residual force and applied load at node  $i$ , respectively. In order for a structure to be in equilibrium, the magnitude of the residual force must vanish at every free node, i.e.

$$\|\mathbf{r}_i\|_2 = 0, \quad \forall i \in \mathcal{S}_{\text{free}}, \quad \mathcal{S}_{\text{free}} := \{i \mid \hat{s}_i < 0\}. \quad (9)$$

To prevent non-equilibrium structures, we apply a post-processing optimization step. Specifically, we perform a

combined optimization of  $\hat{\mathbf{x}}$  and  $\hat{\mathbf{q}}$  and minimize the squared residual force magnitudes of free nodes:

$$\begin{aligned} \min_{\hat{\mathbf{x}}, \hat{\mathbf{q}}} \quad & \sum_{i \in \mathcal{S}_{\text{free}}} \left\| \mathbf{p}_i + \sum_{j \in \mathcal{N}(i)} \tilde{q}_{ij} (\hat{\mathbf{x}}_j - \hat{\mathbf{x}}_i) \right\|_2^2 \\ \text{s.t.} \quad & \hat{\mathbf{x}}_i - \Delta_x \leq \hat{\mathbf{x}}_i \leq \hat{\mathbf{x}}_i + \Delta_x, \quad \forall i, \\ & \hat{q}_{ij} - \Delta_q \leq \tilde{q}_{ij} \leq \hat{q}_{ij} + \Delta_q, \quad \forall (i, j) \in \mathcal{E}. \end{aligned} \quad (10)$$

We initialize  $\hat{\mathbf{x}}$  and  $\hat{\mathbf{q}}$  as the decoder outputs  $\hat{\mathbf{x}}$  and  $\hat{\mathbf{q}}$ , and apply bounds around this initialization defined by  $\Delta_x$  and  $\Delta_q$ . We find that typically only minor adjustments to both  $\hat{\mathbf{x}}$  and  $\hat{\mathbf{q}}$  are needed to obtain structures that are in equilibrium within a given tolerance and set  $\Delta_x = 2$  m and  $\Delta_q = 1$  kN/m to prevent the optimization from straying too far from the decoder prediction. Optionally, any small residual still remaining after optimization can be eliminated by applying a final form-finding step with the Force Density Method (FDM) [55].

### 3.3. Diffusion Transformer

After training the VGAE, we freeze its weights and treat its encoder and decoder as mappings between equilibrium structures and latents  $\mathbf{z}$ . Using this fixed latent space, we can model its distribution using a Gaussian diffusion framework, allowing pure noise to be mapped to the target latent distribution (Figure 4). Specifically, we use a flow-matching formulation that models the transformation from the Gaussian prior to the latent distribution as a time-dependent vector field [57]. In this way, the diffusion process spans the gap between a structure sampled from the gaussian prior using only the VGAE decoder (Figure 4, left), to a structure sampled from an approximation of the actual VGAE latent space (Figure 4, right).

Given an equilibrium structure, we encode it to a target latent  $\mathbf{z}^{(1)}$  at time  $t = 1$ . We sample an initial noise latent  $\mathbf{z}^{(0)}$  from a standard normal, and construct a linearly interpolated latent at a random time  $t \sim \mathcal{U}(0 + \epsilon, 1 - \epsilon)$  via

$$\mathbf{z}^{(t)} = (1 - t) \mathbf{z}^{(0)} + t \mathbf{z}^{(1)}, \quad (11)$$

where we set  $\epsilon = 0.01$  for numerical stability. Along this straight-line path, the ground-truth conditional vector field is

$$u_t(\mathbf{z}^{(t)} \mid \mathbf{z}^{(1)}) = \frac{\mathbf{z}^{(1)} - \mathbf{z}^{(t)}}{1 - t}. \quad (12)$$

The central idea behind flow-matching is to train a neural network to approximate this vector field conditional on  $t$ . During inference, starting with a noise sample we can then integrate along the approximate vector field to arrive at a denoised latent, as depicted by the green line in Figure 4.

To improve training stability, we follow Yim et al. [58] and reparameterize the flow-matching loss to predict the denoised latent according to

$$\mathcal{L}_{\text{fm}} = \frac{1}{N} \sum_{i=1}^N \left\| \frac{\mathbf{z}_i^{(1)} - \mathbf{z}_i^{(t)}}{1 - t} - \frac{\hat{\mathbf{z}}_i^{(1)} - \mathbf{z}_i^{(t)}}{1 - t} \right\|_2^2, \quad (13)$$

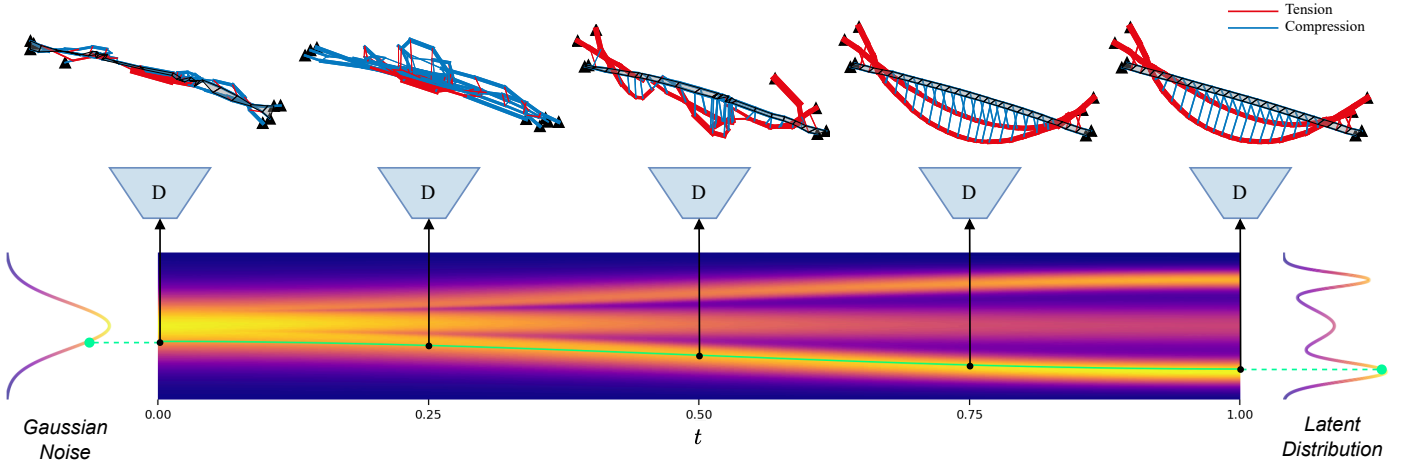


Figure 4: A random sample from a Gaussian distribution is iteratively denoised to a point in the latent space distribution. The VGAE decoder can decode denoised and intermediate samples into structures. Only structures decoded at the end of the diffusion process (right) will be close to an equilibrium state.

which simplifies to

$$\mathcal{L}_{\text{fm}} = \frac{1}{(1-t)^2} \cdot \frac{1}{N} \sum_{i=1}^N \left\| \mathbf{z}_i^{(1)} - \hat{\mathbf{z}}_i^{(1)} \right\|_2^2 \quad (14)$$

in which we clip  $t$  to 0.9 for numerical stability.

For the neural network we use a Diffusion Transformer (DiT) [59]. To guide the diffusion process towards structures that match a given text prompt, we obtain a conditioning vector  $\mathbf{c}$  from a pre-trained CLIP model [60]. We use the OpenCLIP implementation [61] with the ViT-g/14 checkpoint trained on LAION-2B [62]. Conditioning on  $\mathbf{c}$  and  $t$  is injected into the DiT via adaptive layer normalization with zero-initialization.

We train the DiT with  $\mathcal{L}_{\text{fm}}$  in Equation (14), using the frozen VGAE decoder to obtain the target  $\mathbf{z}_i^{(1)}$ . We randomly drop  $\mathbf{c}$  in favor of a learned null embedding  $\varphi$  10% of the time during training, allowing us to apply Classifier-Free Guidance (CFG) [63] during inference, resulting in improved prompt-adherence. Further details and hyperparameters of the DiT can be found in Appendix A.

At inference, we first sample  $\mathbf{z}^{(0)} \sim \mathcal{N}(0, I)$  and integrate the learned vector field forward in time with  $T$  steps of size  $\Delta t = 1/T$ , where we set  $T = 100$ . Using CFG, we evaluate both a conditional and an unconditional DiT pass and combine them to amplify the direction associated with the text embedding:

$$\begin{aligned} \hat{\mathbf{z}}_{\text{cond}}^{(1)} &= \text{DiT}(\mathbf{z}^{(t)}, t, \mathbf{c}, \mathcal{E}), \\ \hat{\mathbf{z}}_{\text{uncond}}^{(1)} &= \text{DiT}(\mathbf{z}^{(t)}, t, \varphi, \mathcal{E}), \\ \hat{\mathbf{z}}^{(1)} &= (1 - \gamma) \hat{\mathbf{z}}_{\text{uncond}}^{(1)} + \gamma \hat{\mathbf{z}}_{\text{cond}}^{(1)}, \end{aligned} \quad (15)$$

in which  $\gamma$  is the guidance scale, which we set to 5.0. We apply a simple Euler integration scheme according to the pseudocode

in Algorithm 1. Finally, after  $T$  steps we decode the denoised latent to an equilibrium structure with the frozen VGAE decoder, and apply the residual force post-optimization from Section 3.2.

---

#### Algorithm 1: Latent Diffusion Euler Sampling

---

**Input:** Text embedding  $\mathbf{c}$ , number of steps  $T$ , guidance scale  $\gamma$ , edge set  $\mathcal{E}$   
**Output:** Equilibrium structure  $(\hat{\mathbf{q}}, \hat{\mathbf{x}}, \hat{\mathbf{s}})$

- 1 Sample initial noise:  $\mathbf{z}^{(0)} \sim \mathcal{N}(0, I)$ ;
- 2 Set step size  $\Delta t = 1/T$ ;
- 3 **for**  $t \in \text{linspace}(0, 1, T)$  **do**
- 4      $\hat{\mathbf{z}}_{\text{cond}}^{(1)} = \text{DiT}(\mathbf{z}^{(t)}, t, \mathbf{c}, \mathcal{E})$ ;
- 5      $\hat{\mathbf{z}}_{\text{uncond}}^{(1)} = \text{DiT}(\mathbf{z}^{(t)}, t, \varphi, \mathcal{E})$ ;
- 6      $\hat{\mathbf{z}}^{(1)} = (1 - \gamma) \hat{\mathbf{z}}_{\text{uncond}}^{(1)} + \gamma \hat{\mathbf{z}}_{\text{cond}}^{(1)}$ ;
- 7      $\mathbf{z}^{(t+\Delta t)} = \mathbf{z}^{(t)} + \Delta t \frac{\hat{\mathbf{z}}^{(1)} - \mathbf{z}^{(t)}}{1 - t}$ ;
- 8 **end**
- 9 Decode:  $(\hat{\mathbf{q}}, \hat{\mathbf{x}}, \hat{\mathbf{s}}) = \text{D}(\mathbf{z}^{(1)}, \mathcal{E})$ ;
- 10 Residual force optimization:  $(\hat{\mathbf{q}}, \hat{\mathbf{x}}) = \text{Optim}(\hat{\mathbf{q}}, \hat{\mathbf{x}}, \hat{\mathbf{s}})$ ;

---

#### 3.4. Topology Model

The final neural network of Text2Structure3D is a multilayer perceptron (MLP) that predicts a topology of the structure given the text embedding  $\mathbf{c}$ . During inference, the MLP is the first model to be run following the text embedding model, so that the DiT and VGAE can use the predicted topology for their positional encodings and message passing layers (Appendix A).

Large groups of structures can all share the same topology through variation in their geometry and internal forces, or even their typologies, as is the case for arch and suspension bridges. We make use of this fact to efficiently parameterize all the topologies in our dataset using a limited number of

parameters. This allows us to use a simple MLP to model the distribution of these topology parameters from  $\mathbf{c}$ . We train the MLP using a Cross Entropy (CE) loss, which converges to the topology parameter probability distribution conditional on  $\mathbf{c}$ . Then, during inference, we can sample from this distribution to construct the predicted topology. For additional architecture and hyperparameter details of the MLP we also refer to Appendix A.

### 3.5. Synthetic Dataset

To train Text2Structure3D, we develop a cross-typological synthetic training dataset of equilibrium structures and corresponding text labels (Figure 5). The dataset consists of a combination of funicular arch and suspension bridge structures and statically determinate truss systems.

Funicular structures are form-found with the Combinatorial Equilibrium Modeling (CEM) [35]. By varying the CEM input parameters we can obtain arch and suspension bridge structures with various topologies, geometries and force configurations. Some of the parameters we set include the span, deck width and number of cables or columns along the deck. Bridges either have a single or double arch/cable configuration, for arch and suspension structures respectively. In the case of a double arch/cable configuration, these can be separate or interconnected by additional horizontal members. The deck can be twisted in the horizontal plane and/or cambered vertically and we allow various support configurations that have the arch(es) or main cable(s) above, below, or intersect the deck. During data generation, we sample these form-finding parameters from relatively large bounds so as to maximize the variety of structural configurations in the dataset. To prevent any unrealistic or otherwise undesired structures, we filter out any structures that exceed a specified bounding box, exceed a maximum force density threshold or bend too sharply in the case of twisted bridges.

Truss structures are generated using a parametric model that is purely based on geometric rules. We include Pratt, Howe and Parker truss configurations and allow the trusses to be above (through truss), or below (deck truss) the deck. Similar to funicular bridges we vary the span, deck width and number of bays. The trusses on both sides of the deck can be either vertical, or inclined outwards or inwards. Furthermore, for deck trusses we include a triangular truss configuration such that trusses on either side are connected, sharing the same bottom chord. Finally, to determine the internal member forces we assemble and solve for the global equilibrium matrix.

We apply a canonical orientation to all structures, setting the midspan at the height of the deck to the origin and aligning the deck along the x-axis. We apply a constant line load of 5 kN/m to each bridge, such that during inference it is possible to derive the load from the span of the generated geometry.

To generate text labels, we use a randomized template that combines a list of attributes of each bridge in a description. We include both quantitative attributes, such as span length, deck

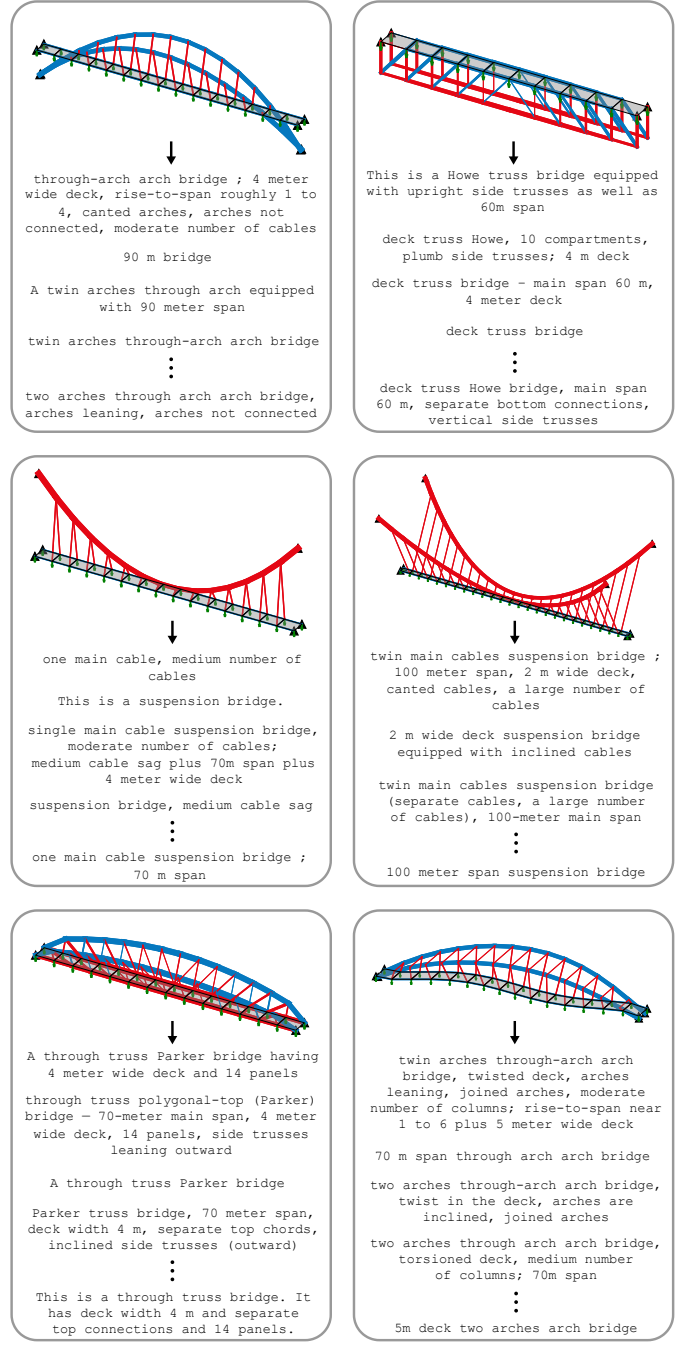


Figure 5: Samples from the cross-typological synthetic training dataset used to train Text2Structure3D. For every equilibrium structure we generate a number of text descriptions of various level of detail.

width and the number of bays, as well as qualitative attributes, such as typology or whether the bridge is twisted. For some attributes we include both quantitative and qualitative descriptions. For example, an arch rise can be described as an exact ratio (e.g. 1:5), or qualitatively (e.g. shallow). We generate text labels with a broad range of level of detail, including descriptions that contain all known attributes of the structure as well as descriptions with only a subset or even just a single one

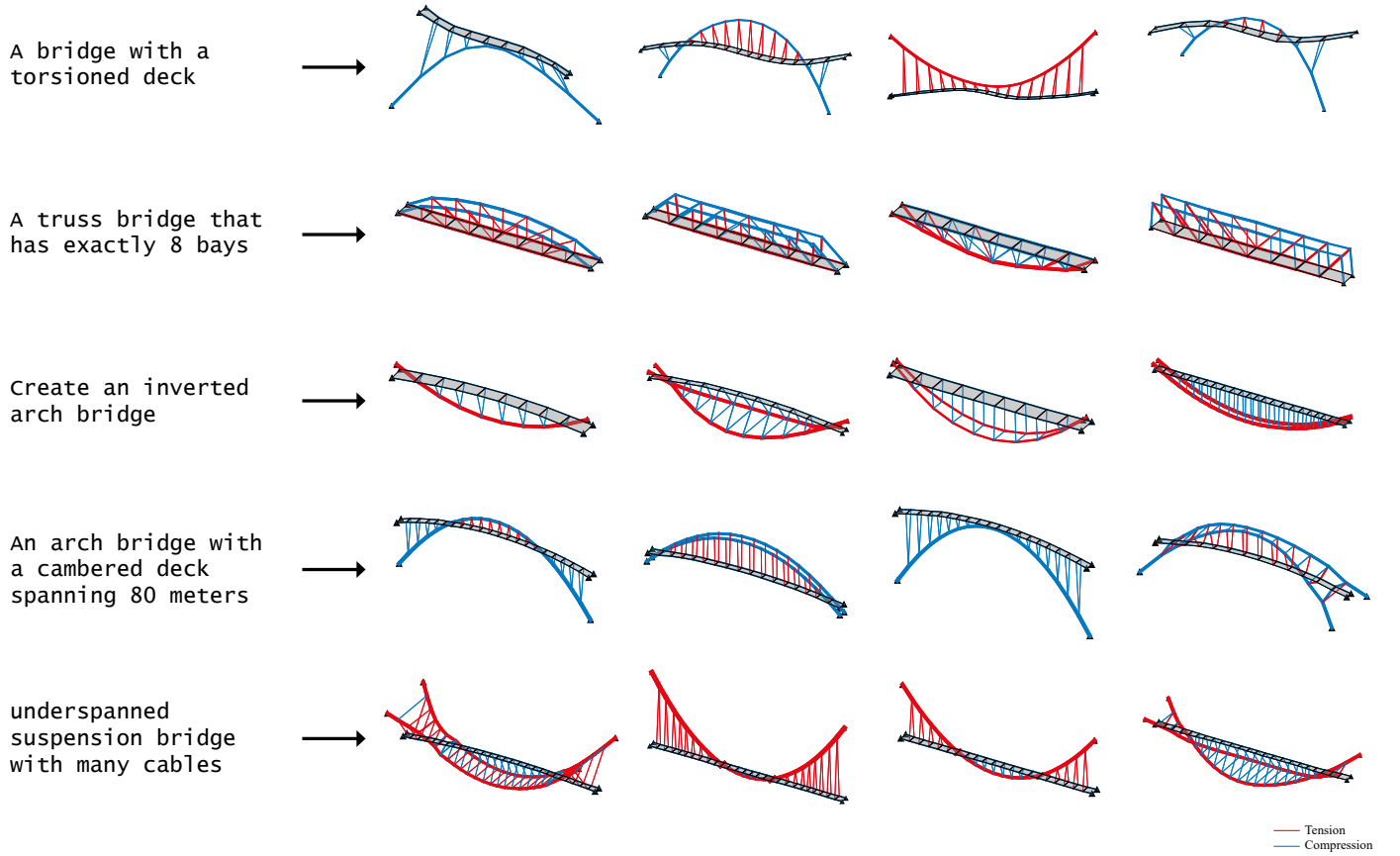


Figure 6: Equilibrium structures generated by Text2Structure3D using various text prompts. Text2Structure3D can generate diverse structures while maintaining adherence to the prompt specifications.

(e.g. a 60 meter span bridge). In this way, we facilitate both use cases in which Text2Structure3D could be prompted with a very detailed description, or a shorter simple request.

We generate 20,000 funicular structures and 10,000 truss structures and combine these into a single dataset of 30,000 structures (Table 1). For each structure we generate 10 unique text labels such that our dataset contains 300,000 structure-text pairs. Finally, we split our data into an 80% training set (24,000) and set aside 20% (6,000) for testing.

Structure Type	# Structures	Labels/Structure	# Pairs
Funicular	20,000	10	200,000
Truss	10,000	10	100,000
Total	30,000	–	300,000

Table 1: Dataset composition of funicular and truss structures with corresponding text labels.

## 4. Results

After training, Text2Structure3D is able to generate a structure of a bridge in equilibrium solely from an input text prompt (Figure 6). As a visual validation, we find generated structures to

be geometrically similar to the training dataset of bridge structures and that prompt specifications are satisfied. Generated structures are consistently of the requested topology and qualitative attributes such as *a torsioned deck* are satisfied as well. To evaluate the results quantitatively we study the reconstruction performance (Section 4.1) as well as the quantitative prompt adherence (Section 4.2) in more detail.

### 4.1. Reconstruction

We evaluate reconstructions in two ways, by assessing if they are in equilibrium, and according to their geometric reconstruction error. Reconstructed structures should be in equilibrium, which we measure by the residual force error  $\epsilon_{\text{residual}}$ , calculated as the average residual force magnitude among free nodes:

$$\epsilon_{\text{residual}} = \frac{1}{|\mathcal{S}_{\text{free}}|} \sum_{i \in \mathcal{S}_{\text{free}}} \|r_i\|_2, \quad (16)$$

where  $\epsilon_{\text{residual}} = 0$  corresponds to a structure in equilibrium.

The simplest way to obtain a reconstructed structure in equilibrium is by applying the Force Density Method (FDM) directly

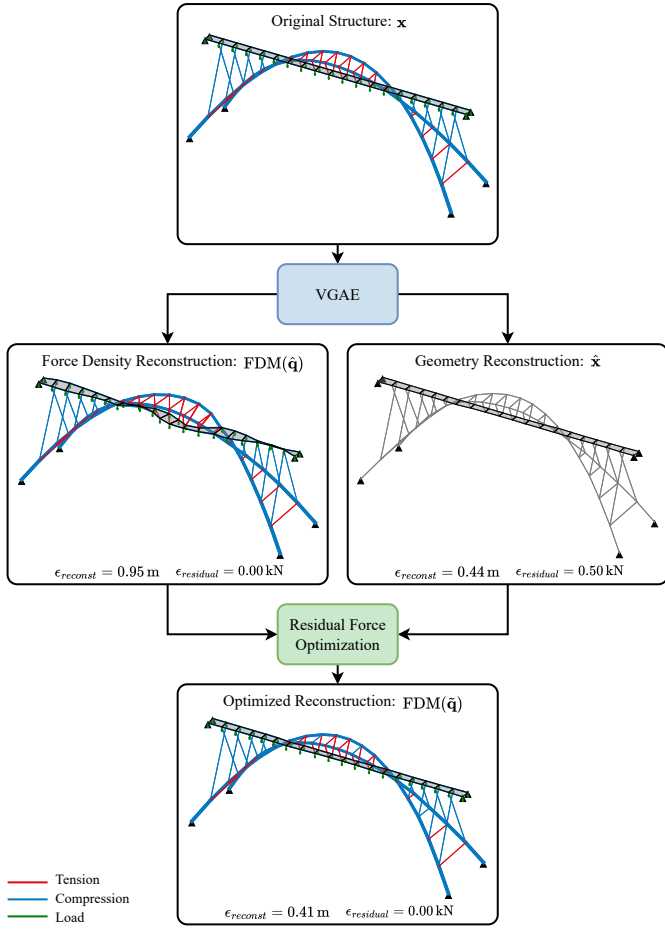


Figure 7: Variational Graph Auto-encoder (VGAE) reconstructions before and after residual force optimization. Force density-based reconstructions are guaranteed to be in equilibrium ( $\epsilon_{\text{residual}} = 0$ ), while geometry-based reconstructions have a lower reconstruction error ( $\epsilon_{\text{reconst}}$ ). We obtain a structure that combines the advantages of both by applying a residual force optimization post-processing step.

to the predicted  $\hat{\mathbf{q}}$  produced by the VGAE (Figure 7, left). However, the geometry produced by the FDM is very sensitive to small perturbations of  $\hat{\mathbf{q}}$ , which can result in asymmetric structures that are visually dissimilar to the original. We measure the quality of the reconstructed geometry using a reconstruction error  $\epsilon_{\text{reconst}}$ , defined as the average nodal distance to the original structure:

$$\epsilon_{\text{reconst}} = \frac{1}{N} \sum_{i=1}^N \|\hat{\mathbf{x}}_i - \mathbf{x}_i\|_2, \quad (17)$$

We find direct geometry predictions (Figure 7, right) to have a significantly lower  $\epsilon_{\text{reconst}}$ , though they are not in equilibrium, having a non-zero  $\epsilon_{\text{residual}}$ . Our combined optimization can typically find an equilibrium geometry close to  $\hat{\mathbf{x}}$  with minimal changes to  $\hat{\mathbf{q}}$  (Figure 7, bottom). Comparing the pure force density-based reconstruction and the optimization-based reconstruction across the test set we find a consistent reduction in  $\epsilon_{\text{reconst}}$  (Figure 8). The optimization reduces the median  $\epsilon_{\text{reconst}}$  from 0.90 m to 0.47 m. Due to the long tail in the pre-

optimization distribution of  $\epsilon_{\text{reconst}}$  the mean is reduced even more drastically, from 2.96 m to 0.61 m.

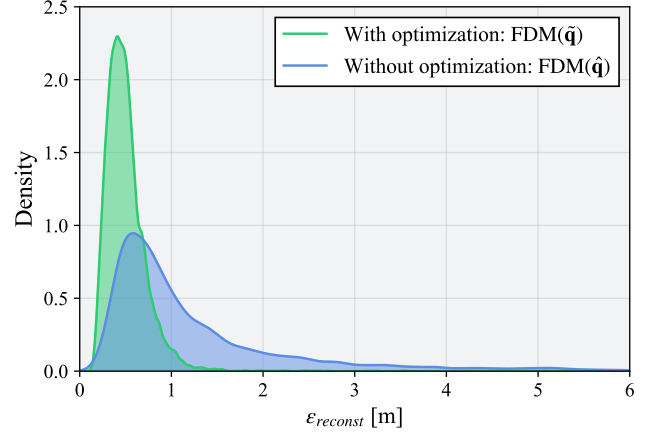


Figure 8: Probability density function of the reconstruction error ( $\epsilon_{\text{reconst}}$ ) for force density-based reconstructions (without optimization) and for reconstructions optimized with a residual force optimization post-processing step.

#### 4.2. Prompt Adherence

To evaluate the prompt adherence of Text2Structure3D we study the distributions of measurable attributes of 1000 generated structures for prompts containing specifications for those attributes. For each attribute we evaluate 3 types of prompts: firstly, we use a simple prompt containing a specification for a single attribute, written in a way that is similar to the text labels in the training dataset (Figure 9, first row). Secondly, we evaluate an alternative prompt with the same information as the first, written in a way the model has not encountered during training (second row). Examples include replacing *60* with *sixty*, or using a longer phrase *a span 4 times larger than its rise* instead of *1:4 rise-to-span*. Finally we evaluate the performance on more complex prompts that contain specifications for multiple other attributes as well (third row). We compare each prompt against an unconditional baseline and the test dataset distribution (fourth row). For typology-specific attributes, such as rise-to-span ratio, we compare against the distribution of structures only of the relevant typology instead.

Overall we find generated structures to adhere to the prompt, with distributions significantly concentrated around the request. Comparing this to unconditional or typology-only conditional generation we find a much broader distribution of attributes. Distributions are mostly symmetric around the request, with the exception of the simple prompt for the rise-to-span ratio which has a significant bias to the left. In general, we observe a higher variance for the continuous attributes than we do for discrete attributes like the number of bays.

The alternative prompt distributions are marginally worse than those of the simple prompt, indicating robustness against the resulting changes in text embeddings obtained from CLIP. Complex prompt are also only marginally worse, indicating

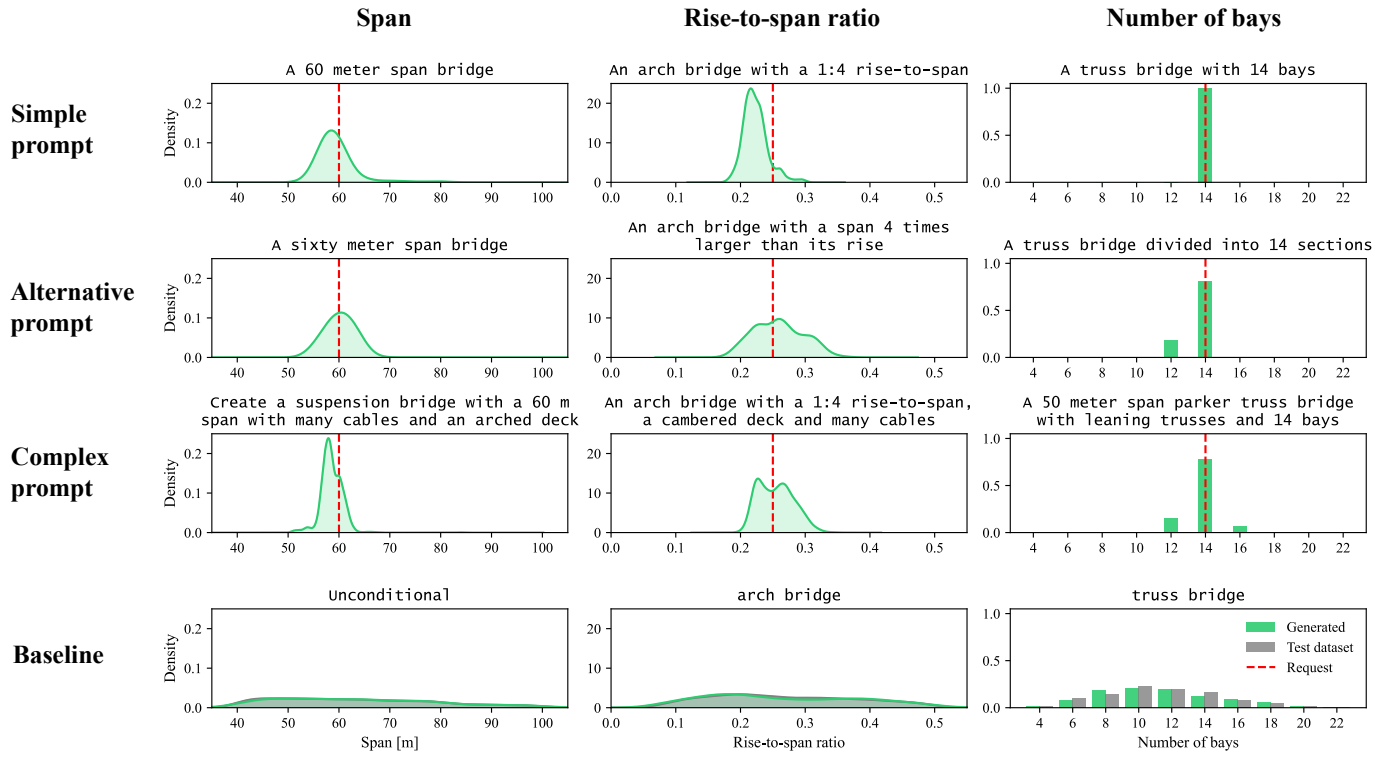


Figure 9: Distributions of generated structures for prompts containing specifications for the span (left), rise-to-span ratio (center) and number of bays (right). For each we evaluate a simple prompt similar to the dataset labels (first row), an alternative prompt worded in a way the model has not encountered during training (second row), and a complex prompt containing multiple requests (third row). As a baseline we evaluate unconditional generation compared to the test dataset distribution (fourth row). For each prompt we show a kernel density estimation or categorical probability distribution derived from 1000 generated samples.

the model is capable of parsing multiple specifications accurately. Finally, we see that unconditional and typology-only conditional generation tightly matches the distribution of the test dataset.

## 5. Discussion

### 5.1. Limitations

Text2Structure3D significantly advances the ability for the generative modeling of equilibrium structures, yet a number of important limitations remain.

Firstly, while we strived to make our dataset as diverse as possible, we limited the scope of data generation to a reasonable number of bridge typologies. While Text2Structure3D has been designed with the application to more general datasets in mind, a number of aspects of the model still make use of the limited level of complexity of the dataset presented in this work.

One such limitation is the parametric model-based approach for the topology MLP. Similar to previous research, this part of Text2Structure3D will face challenges in scalability for more general datasets. Additionally, the fact that our dataset only contained bridge structures with a single load case allowed us to derive the loading condition from the generated geometry. A more general dataset would likely require an explicit modeling

of the external load as well. Finally, our model has been trained on structures that are zero-centered with the deck aligned along the x-axis, whereas such a canonical orientation might not be available for a more general class of structures.

### 5.2. Future Work

Primary directions for future work include the creation of a broader dataset of equilibrium structures and adapting the generative modeling strategies presented in this work to accommodate such a dataset.

We repeat the common notion in the AEC industry that dataset availability is a key bottleneck to developing ML applications. In the context of this work, a more general dataset of bridge structures containing more typologies such as cable-stayed or cantilever bridges would already make the presented model more powerful. It is also likely the model would benefit from richer and more various text labels. Additional quantitative attributes could be assigned with Finite Element Method (FEM) analyses and additional qualitative and subjective attributes could be included using data labeling strategies based on clustering techniques such as Self-Organizing Maps (SOM) [24, 26]. Beyond the information included in the text labels, more varied wording could be achieved using LLMs to further increase the robustness of the model. An additional use of LLMs could be the implementation of Text2Structure3D

in an agentic framework, expanding the ways in which users can interact with the model. Furthermore, another opportunity for enhancing user interactions with the model is to include explainable AI techniques, though also this is beyond the scope of the current work.

Development of a more general dataset containing typologies beyond bridge structures would need to be accompanied by advances in a few key areas of the generative modeling strategy as well. Most notably, potential alternatives for the parametric model-based strategy for predicting the topology include ground structure-based approaches, similar to link prediction applications, or autoregressive approaches, for example using reinforcement learning. To overcome the challenges of training on datasets without a clear canonical orientation, Equivariant Graph Neural Networks (EGNN) could provide a solution [41].

Finally, while in this work we focused on conditioning generation on structures, the presented model architecture is compatible with other types of modalities for conditioning as well. Most prominently, this opens the opportunity for generating structures from images, such as design sketches, screenshots of 3D models or even photos of existing structures.

## 6. Conclusion

We presented Text2Structure3D, a graph-based generative model for equilibrium structures based on latent diffusion conditioned on natural language. Text2Structure3D allows the generation of graph-based structures of various topology, geometry and force configuration, greatly improving the generalization abilities of existing generative approaches built around parametric models in structural design. To train Text2Structure3D, we developed a cross-typological dataset of bridge structures combined with text descriptions as labels. Generated structures show strong adherence to the specifications in the text prompt, even when provided with prompts containing multiple attribute specifications or alternative wording to the prompts in the training dataset. To adapt latent diffusion for equilibrium structures, we introduce a residual force optimization step that can guarantee predicted structures are in equilibrium while improving reconstruction performance. Current limitations include the limited scope of the training dataset and the parametric model-based approach for topology predictions. Looking ahead, by addressing these limitations Text2Structure3D could have the potential of forming the basis for a general-purpose foundation model for structural design applications.

## Declaration of Competing Interest

The authors declare that they have no known competing financial interests or personal relationships that could have appeared to influence the work reported in this paper.

## Declaration of Generative AI and AI-assisted technologies in the writing process

During the preparation of this work the author(s) used large language models in order to improve sentence structure. After using this tool/service, the author(s) reviewed and edited the content as needed and take(s) full responsibility for the content of the publication.

## Acknowledgments

This work is supported in part by the International Graduate School of Science and Engineering (IGSSE) of the Technical University of Munich (TUM). The authors gratefully acknowledge the NVIDIA AI Technology Center at the University of Florida for its technical support and for granting access to computing resources.

## Appendix A. Implementation Details

**Variational Graph Auto-Encoder.** The VGAE [7] decoder and encoder are based on a graph transformer as described by Rampasek et al. [56]. For the message passing layer we use a GINE convolution [64], and for global attention a standard Transformer encoder block [65] with 4 attention heads. We set the latent dimension  $d_z = 8$  and use 9 layers with hidden dimension  $d_h = 128$ . We train the VGAE for 3 days on a single NVIDIA RTX 6000 Ada GPU with Adam [66] using a learning rate of  $1e - 4$  and a batch size  $b = 128$ .

**Diffusion Transformer** We use a largely unmodified DiT architecture [6] using 12 layers with a hidden dimension  $d_h = 1536$  and 24 attention heads. We use both general graph positional and structural encodings, as well as positional encodings specific to our dataset. For general encodings we apply Laplacian Positional Encodings (LPE) [67] using 12 eigenvectors and Random-Walk Structural Encodings (RWSE) [68] using 12 random walks. For bridge-specific encodings we add integer indicators for nodes being part of the deck or not, on which side of the bridge they belong to—both along and orthogonal to the span—and the shortest n-hop distance to one of the supports. We train the DiT on the same hardware as the VGAE also for 3 days with Adam using a learning rate of  $1e - 4$  and a batch size  $b = 64$ .

**Topology MLP.** The Topology MLP consists of 2 layers with a hidden dimension  $d_h = 512$  followed by a ReLU activation function [69] and a dropout rate of 0.1. We use Adam with a learning rate of  $1e - 3$  with a batch size of  $b = 128$  and train the MLP for 20 minutes on an NVIDIA RTX 4080 which we found to be sufficient for the model to converge.

## References

- [1] S. Kaethner, J. Burridge, Embodied CO2 of structural frames, *The Structural Engineer* 90 (5) (2012) 33–40. doi:<https://doi.org/10.56330/RDKY7745>.

[2] B. C. Paulson, Designing to reduce construction costs, *Journal of the Construction Division* 102 (4) (1976) 587–592. doi:[10.1061/JCCEAZ.0000639](https://doi.org/10.1061/JCCEAZ.0000639).

[3] X. Zhuang, P. Zhu, A. Yang, L. Caldas, Machine learning for generative architectural design: Advancements, opportunities, and challenges, *Automation in Construction* 174 (2025) 106129. doi:<https://doi.org/10.1016/j.autcon.2025.106129>.

[4] R. E. Weber, C. Mueller, C. Reinhart, Automated floor-plan generation in architectural design: A review of methods and applications, *Automation in Construction* 140 (2022) 104385. doi:<https://doi.org/10.1016/j.autcon.2022.104385>.

[5] C. Du, S. Esser, S. Nousias, A. Borrmann, Text2bim: Generating building models using a large language model-based multi-agent framework, *arXiv preprint* (2025). arXiv:2408.08054.

[6] R. Rombach, A. Blattmann, D. Lorenz, P. Esser, B. Ommer, High-resolution image synthesis with latent diffusion models, in: *Proceedings of the IEEE/CVF Conference on Computer Vision and Pattern Recognition (CVPR)*, 2022, pp. 10684–10695.  
URL [https://openaccess.thecvf.com/content/CVPR2022/html/Rombach\\_High-Resolution\\_Image\\_Synthesis\\_With\\_Latent\\_Diffusion\\_Models\\_CVPR\\_2022\\_paper.html](https://openaccess.thecvf.com/content/CVPR2022/html/Rombach_High-Resolution_Image_Synthesis_With_Latent_Diffusion_Models_CVPR_2022_paper.html)

[7] T. N. Kipf, M. Welling, Variational graph auto-encoders, *arXiv preprint* (2016). arXiv:1611.07308.

[8] V. P. Dwivedi, X. Bresson, A generalization of transformer networks to graphs, *arXiv preprint* (2020). arXiv:2012.09699.

[9] K. Shea, R. Aish, M. Gourtovaia, Towards integrated performance-driven generative design tools, *Automation in Construction* 14 (2) (2005) 253–264. doi:<https://doi.org/10.1016/j.autcon.2004.07.002>.

[10] S. Krish, A practical generative design method, *Computer-Aided Design* 43 (1) (2011) 88–100. doi:<https://doi.org/10.1016/j.cad.2010.09.009>.

[11] R. Woodbury, *Elements of Parametric Design*, Routledge, New York, 2010.

[12] K. Shea, J. Cagan, Languages and semantics of grammatical discrete structures, *Artificial Intelligence for Engineering Design, Analysis and Manufacturing* 13 (4) (1999) 241–251. doi:<https://doi.org/10.1017/S0890060499134012>.

[13] D. Veenendaal, P. Block, An overview and comparison of structural form finding methods for general networks, *International Journal of Solids and Structures* 49 (26) (2012) 3741–3753. doi:<https://doi.org/10.1016/j.ijsolstr.2012.08.008>.

[14] M. P. Bendsøe, N. Kikuchi, Generating optimal topologies in structural design using a homogenization method, *Computer Methods in Applied Mechanics and Engineering* 71 (2) (1988) 197–224. doi:[https://doi.org/10.1016/0045-7825\(88\)90086-2](https://doi.org/10.1016/0045-7825(88)90086-2).

[15] W. S. Dorn, R. E. Gomory, H. J. Greenberg, Automatic design of optimal structures, *Journal de Mécanique* 3 (1964) 25–52.

[16] D. E. Goldberg, *Genetic Algorithms in Search, Optimization, and Machine Learning*, Addison-Wesley, Reading, MA, 1989.

[17] P. Hajela, E. Lee, Genetic algorithms in truss topological optimization, *International Journal of Solids and Structures* 32 (22) (1995) 3341–3357. doi:[https://doi.org/10.1016/0020-7683\(94\)00306-H](https://doi.org/10.1016/0020-7683(94)00306-H).

[18] N. C. Brown, C. T. Mueller, Design variable analysis and generation for performance-based parametric modeling in architecture, *International Journal of Architectural Computing* 17 (1) (2019) 36–52. doi:[10.1177/1478077118799491](https://doi.org/10.1177/1478077118799491).

[19] D. P. Kingma, M. Welling, Auto-encoding variational bayes, *arXiv preprint* (2013). arXiv:1312.6114.

[20] R. Danhaive, C. T. Mueller, Design subspace learning: Structural design space exploration using performance-conditioned generative modeling, *Automation in Construction* 127 (2021) 103664. doi:<https://doi.org/10.1016/j.autcon.2021.103664>.

[21] M. J. J. Bucher, M. A. Kraus, R. Rust, S. Tang, Performance-based generative design for parametric modeling of engineering structures using deep conditional generative models, *Automation in Construction* 156 (2023) 105128. doi:<https://doi.org/10.1016/j.autcon.2023.105128>.

[22] A. Adadi, M. Berrada, Peeking inside the black-box: A survey on explainable artificial intelligence (xai), *IEEE Access* 6 (2018) 52138–52160. doi:<https://doi.org/10.1109/ACCESS.2018.2870052>.

[23] V. Balmer, S. V. Kuhn, R. Bischof, L. Salamanca, W. Kaufmann, F. Perez-Cruz, M. A. Kraus, Design space exploration and explanation via conditional variational autoencoders in meta-model-based conceptual design of pedestrian bridges, *Automation in Construction* 163 (2024) 105411. doi:<https://doi.org/10.1016/j.autcon.2024.105411>.

[24] K. S. Ochoa, P. O. Ohlbrock, P. D'Acunto, V. Moosavi, Beyond typologies, beyond optimization: Exploring novel structural forms at the interface of human and machine intelligence, *International Journal of Architectural Computing* 19 (3) (2021) 466–490. doi:<https://doi.org/10.1177/1478077120943062>.

[25] I. Goodfellow, J. Pouget-Abadie, M. Mirza, B. Xu, D. Warde-Farley, S. Ozair, A. Courville, Y. Bengio, Generative adversarial nets, in: Advances in Neural Information Processing Systems, Vol. 27, 2014, pp. 2672–2680.  
URL [https://proceedings.neurips.cc/paper\\_files/paper/2014/file/f033ed80deb0234979a61f95710dbe25-Paper.pdf](https://proceedings.neurips.cc/paper_files/paper/2014/file/f033ed80deb0234979a61f95710dbe25-Paper.pdf)

[26] Z. Guo, K. Saldana Ochoa, P. D'Acunto, Enhancing structural form-finding through a text-based ai engine coupled with computational graphic statics, in: Innovation, Sustainability and Legacy, International Association for Shell and Spatial Structures, Beijing, China, 2022.  
URL <https://www.ingentaconnect.com/content/iass/piass/2022/00002022/00000008/art00013>

[27] W. Liao, X. Lu, Y. Huang, Z. Zheng, Y. Lin, Automated structural design of shear wall residential buildings using generative adversarial networks, Automation in Construction 132 (2021) 103931. doi:<https://doi.org/10.1016/j.autcon.2021.103931>.

[28] G. Mirra, A. Pugnale, Comparison between human-defined and ai-generated design spaces for the optimisation of shell structures, Structures 34 (2021) 2950–2961. doi:<https://doi.org/10.1016/j.istruc.2021.09.058>.

[29] K.-M. M. Tam, P. D'Acunto, N. C. Brown, L. Bleker, T. Van Mele, P. Block, A unified differentiable geometric deep learning message passing framework for inverse structural form-finding, SSRN preprint (2025). doi:<https://doi.org/10.2139/ssrn.5316084>.

[30] K.-H. Chang, C.-Y. Cheng, Learning to simulate and design for structural engineering, in: H. D. III, A. Singh (Eds.), Proceedings of the 37th International Conference on Machine Learning, PMLR, 2020, pp. 1426–1436.  
URL <https://proceedings.mlr.press/v119/chang20a.html>

[31] E. Whalen, C. Mueller, Toward reusable surrogate models: Graph-based transfer learning on trusses, Journal of Mechanical Design 144 (2) (2021) 021704. doi:<https://doi.org/10.1115/1.4052298>.

[32] K. Hayashi, M. Ohsaki, Graph-based reinforcement learning for discrete cross-section optimization of planar steel frames, Advanced Engineering Informatics 51 (2022) 101512. doi:<https://doi.org/10.1016/j.aei.2021.101512>.

[33] K. Hayashi, M. Ohsaki, M. Kotera, Assembly sequence optimization of spatial trusses using graph embedding and reinforcement learning, Journal of the International Association for Shell and Spatial Structures 63 (4) (2022) 232–240. doi:<https://doi.org/10.20898/j.iass.2022.016>.

[34] P. Zhao, W. Liao, Y. Huang, X. Lu, Intelligent design of shear wall layout based on graph neural networks, Advanced Engineering Informatics 55 (2023) 101886. doi:<https://doi.org/10.1016/j.aei.2023.101886>.

[35] P. O. Ohlbrock, P. D'Acunto, A computer-aided approach to equilibrium design based on graphic statics and combinatorial variations, Computer-Aided Design 121 (2020) 102802. doi:<https://doi.org/10.1016/j.cad.2019.102802>.

[36] L. Bleker, R. Pastrana, P. O. Ohlbrock, P. D'Acunto, Structural form-finding enhanced by graph neural networks, in: C. Gengnagel, O. Baverel, G. Betti, M. Popescu, M. R. Thomsen, J. Wurm (Eds.), Towards Radical Regeneration: Design Modelling Symposium, Springer International Publishing, Berlin, Germany, 2022, pp. 24–35. doi:[https://doi.org/10.1007/978-3-031-13249-0\\_3](https://doi.org/10.1007/978-3-031-13249-0_3).

[37] L. Bleker, K.-M. M. Tam, P. D'Acunto, Logic-informed graph neural networks for structural form-finding, Advanced Engineering Informatics 61 (2024) 102510. doi:<https://doi.org/10.1016/j.aei.2024.102510>.

[38] K.-M. M. Tam, T. Van Mele, P. Block, Trans-topological learning and optimisation of reticulated equilibrium shell structures with automatic differentiation and cw complexes message passing, in: Proceedings of IASS Annual Symposia, International Association for Shell and Spatial Structures, Beijing, China, 2022.  
URL <https://www.ingentaconnect.com/content/iass/piass/2022/00002022/00000008/art00031>

[39] K.-M. M. Tam, N. C. Brown, M. Bronstein, T. V. Mele, P. Block, Learning constrained static equilibrium for thrust network inverse form-finding via physics-informed geometric deep learning on cw complexes, Advanced Engineering Informatics 70 (2026) 103870. doi:<https://doi.org/10.1016/j.aei.2025.103870>.

[40] V. G. Satorras, E. Hoogeboom, M. Welling, E(n) equivariant graph neural networks, in: M. Meila, T. Zhang (Eds.), Proceedings of the 38th International Conference on Machine Learning, PMLR, 2021, pp. 9323–9332.  
URL <https://proceedings.mlr.press/v139/satorras21a.html>

[41] L. Bleker, P. D'Acunto, K.-M. M. Tam, Generalized inverse structural form-finding using e(3)-equivariant physics-based graph neural networks, SSRN preprint (2024). doi:<https://doi.org/10.2139/ssrn.5208576>.

[42] W. Liao, X. Lu, Y. Fei, Y. Gu, Y. Huang, Generative ai design for building structures, Automation in Construction 157 (2024) 105187. doi:<https://doi.org/10.1016/j.autcon.2023.105187>.

[43] J. Sohl-Dickstein, E. Weiss, N. Maheswaranathan, S. Ganguli, Deep unsupervised learning using nonequilibrium thermodynamics, in: F. Bach, D. Blei (Eds.), Proceedings of the 32nd International Conference on Machine Learning, PMLR, Lille, France, 2015, pp. 2256–2265.  
 URL <https://proceedings.mlr.press/v37/sohl-dickstein15.html>

[44] J. Ho, A. Jain, P. Abbeel, Denoising diffusion probabilistic models, in: H. Larochelle, M. Ranzato, R. Hadsell, M. Balcan, H. Lin (Eds.), Advances in Neural Information Processing Systems, Curran Associates, Inc., 2020, pp. 6840–6851.  
 URL [https://proceedings.neurips.cc/paper\\_files/paper/2020/file/4c5bcfec8584af0d967f1ab10179ca4b-Paper.pdf](https://proceedings.neurips.cc/paper_files/paper/2020/file/4c5bcfec8584af0d967f1ab10179ca4b-Paper.pdf)

[45] Y. Song, J. Sohl-Dickstein, D. P. Kingma, A. Kumar, S. Ermon, B. Poole, Score-based generative modeling through stochastic differential equations, in: Proceedings of the International Conference on Learning Representations, 2021.  
 URL <https://openreview.net/forum?id=PxTIG12RRHS>

[46] A. Ramesh, P. Dhariwal, A. Nichol, C. Chu, M. Chen, Hierarchical text-conditional image generation with clip latents, arXiv preprint (2022). [arXiv:2204.06125](https://arxiv.org/abs/2204.06125).

[47] Z. Kong, W. Ping, J. Huang, K. Zhao, B. Catanzaro, Diffwave: A versatile diffusion model for audio synthesis, in: Proceedings of the International Conference on Learning Representations, 2021.  
 URL <https://openreview.net/forum?id=a-xFK8Ymz5J>

[48] X. Li, J. Thickstun, I. Gulrajani, P. S. Liang, T. B. Hashimoto, Diffusion-lm improves controllable text generation, in: S. Koyejo, S. Mohamed, A. Agarwal, D. Belgrave, K. Cho, A. Oh (Eds.), Advances in Neural Information Processing Systems, Curran Associates, Inc., 2022, pp. 4328–4343.  
 URL [https://proceedings.neurips.cc/paper\\_files/paper/2022/file/1be5bc25d50895ee656b8c2d9eb89d6a-Paper-Conference.pdf](https://proceedings.neurips.cc/paper_files/paper/2022/file/1be5bc25d50895ee656b8c2d9eb89d6a-Paper-Conference.pdf)

[49] C. Vignac, I. Krawczuk, A. Siraudin, B. Wang, V. Cevher, P. Frossard, Digress: Discrete denoising diffusion for graph generation, in: The Eleventh International Conference on Learning Representations, 2023.  
 URL <https://openreview.net/forum?id=UaAD-Nu86WX>

[50] E. Hoogeboom, V. G. Satorras, C. Vignac, M. Welling, Equivariant diffusion for molecule generation in 3D, in: K. Chaudhuri, S. Jegelka, L. Song, C. Szepesvari, G. Niu, S. Sabato (Eds.), Proceedings of the 39th International Conference on Machine Learning, PMLR, Baltimore, USA, 2022, pp. 8867–8887.  
 URL <https://proceedings.mlr.press/v162/hoogeboom22a.html>

[51] L. Wu, C. Gong, X. Liu, M. Ye, Q. Liu, Diffusion-based molecule generation with informative prior bridges, in: S. Koyejo, S. Mohamed, A. Agarwal, D. Belgrave, K. Cho, A. Oh (Eds.), Advances in Neural Information Processing Systems, Curran Associates, Inc., 2022, pp. 36533–36545.  
 URL [https://proceedings.neurips.cc/paper\\_files/paper/2022/file/eccc6e11878857e87ec7dd109eaa9eeb-Paper-Conference.pdf](https://proceedings.neurips.cc/paper_files/paper/2022/file/eccc6e11878857e87ec7dd109eaa9eeb-Paper-Conference.pdf)

[52] N. Anand, T. Achim, Protein structure and sequence generation with equivariant denoising diffusion probabilistic models, arXiv preprint (2022). [arXiv:2205.15019](https://arxiv.org/abs/2205.15019).

[53] M. Xu, A. S. Powers, R. O. Dror, S. Ermon, J. Leskovec, Geometric latent diffusion models for 3D molecule generation, in: A. Krause, E. Brunskill, K. Cho, B. Engelhardt, S. Sabato, J. Scarlett (Eds.), Proceedings of the 40th International Conference on Machine Learning, PMLR, 2023, pp. 38592–38610.  
 URL <https://proceedings.mlr.press/v202/xu23n.html>

[54] C. K. Joshi, X. Fu, Y.-L. Liao, V. Gharakhanyan, B. K. Miller, A. Sriram, Z. W. Ulissi, All-atom diffusion transformers: Unified generative modelling of molecules and materials, in: A. Singh, M. Fazel, D. Hsu, S. Lacoste-Julien, F. Berkenkamp, T. Maharaj, K. Wagstaff, J. Zhu (Eds.), Proceedings of the 42nd International Conference on Machine Learning, PMLR, 2025, pp. 28393–28417.  
 URL <https://proceedings.mlr.press/v267/joshi25a.html>

[55] H.-J. Schek, The force density method for form finding and computation of general networks, Computer Methods in Applied Mechanics and Engineering 3 (1) (1974) 115–134. doi:[https://doi.org/10.1016/0045-7825\(74\)90045-0](https://doi.org/10.1016/0045-7825(74)90045-0).

[56] L. Rampášek, M. Galkin, V. P. Dwivedi, A. T. Luu, G. Wolf, D. Beaini, Recipe for a general, powerful, scalable graph transformer, in: S. Koyejo, S. Mohamed, A. Agarwal, D. Belgrave, K. Cho, A. Oh (Eds.), Advances in Neural Information Processing Systems, Curran Associates, Inc., 2022, pp. 14501–14515.  
 URL [https://proceedings.neurips.cc/paper\\_files/paper/2022/file/5d4834a159f1547b267a05a4e2b7cf5e-Paper-Conference.pdf](https://proceedings.neurips.cc/paper_files/paper/2022/file/5d4834a159f1547b267a05a4e2b7cf5e-Paper-Conference.pdf)

[57] Y. Lipman, R. T. Q. Chen, H. Ben-Hamu, M. Nickel, M. Le, Flow matching for generative modeling, in: The Eleventh International Conference on Learning

Representations, 2023.

URL <https://openreview.net/forum?id=PqvMRDCJT9t>

[58] J. Yim, A. Campbell, A. Y. K. Foong, M. Gastegger, J. Jiménez-Luna, S. Lewis, V. G. Satorras, B. S. Veeling, R. Barzilay, T. Jaakkola, F. Noé, Fast protein backbone generation with  $se(3)$  flow matching, arXiv preprint (2023). [arXiv:2310.05297](https://arxiv.org/abs/2310.05297).

[59] W. Peebles, S. Xie, Scalable diffusion models with transformers, in: Proceedings of the IEEE/CVF International Conference on Computer Vision (ICCV), 2023, pp. 4195–4205.

[60] A. Radford, J. W. Kim, C. Hallacy, A. Ramesh, G. Goh, S. Agarwal, G. Sastry, A. Askell, P. Mishkin, J. Clark, G. Krueger, I. Sutskever, Learning transferable visual models from natural language supervision, in: M. Meila, T. Zhang (Eds.), Proceedings of the 38th International Conference on Machine Learning, PMLR, 2021, pp. 8748–8763.

URL <https://proceedings.mlr.press/v139/radford21a.html>

[61] G. Ilharco, M. Wortsman, R. Wightman, C. Gordon, N. Carlini, R. Taori, A. Dave, V. Shankar, H. Namkoong, J. Miller, H. Hajishirzi, A. Farhadi, L. Schmidt, Open-clip (v3.2.0) (2021). doi:<https://doi.org/10.5281/zenodo.17171361>.

[62] C. Schuhmann, R. Beaumont, R. Vencu, C. W. Gordon, R. Wightman, M. Cherti, T. Coombes, A. Katta, C. Mullis, M. Wortsman, P. Schramowski, S. R. Kundurthy, K. Crowson, L. Schmidt, R. Kaczmarczyk, J. Jitsev, LAION-5b: An open large-scale dataset for training next generation image-text models, in: Thirty-sixth Conference on Neural Information Processing Systems Datasets and Benchmarks Track, 2022.

URL <https://openreview.net/forum?id=M3Y74vmsMcY>

[63] J. Ho, T. Salimans, Classifier-free diffusion guidance, arXiv preprint (2022). [arXiv:2207.12598](https://arxiv.org/abs/2207.12598).

[64] W. Hu, B. Liu, J. Gomes, M. Zitnik, P. Liang, V. Pande, J. Leskovec, Strategies for pre-training graph neural networks, in: International Conference on Learning Representations, 2020.

URL <https://openreview.net/forum?id=HJ1WWJSFDH>

[65] A. Vaswani, N. Shazeer, N. Parmar, J. Uszkoreit, L. Jones, A. N. Gomez, L. u. Kaiser, I. Polosukhin, Attention is all you need, in: I. Guyon, U. V. Luxburg, S. Bengio, H. Wallach, R. Fergus, S. Vishwanathan, R. Garnett (Eds.), Advances in Neural Information Processing Systems, Curran Associates, Inc., 2017.

URL <https://proceedings.neurips.org>

cc/paper\_files/paper/2017/file/3f5ee243547dee91fdb053c1c4a845aa-Paper.pdf

[66] D. P. Kingma, J. Ba, Adam: A method for stochastic optimization, International Conference on Learning Representations (ICLR) (2015). [arXiv:1412.6980](https://arxiv.org/abs/1412.6980).

[67] V. P. Dwivedi, C. K. Joshi, A. T. Luu, T. Laurent, Y. Bengio, X. Bresson, Benchmarking graph neural networks, Journal of Machine Learning Research 24 (43) (2023) 1–48.

URL <http://jmlr.org/papers/v24/22-0567.html>

[68] V. P. Dwivedi, A. T. Luu, T. Laurent, Y. Bengio, X. Bresson, Graph neural networks with learnable structural and positional representations, in: International Conference on Learning Representations, 2022.

URL <https://openreview.net/forum?id=wTTjnvGphYj>

[69] V. Nair, G. E. Hinton, Rectified linear units improve restricted boltzmann machines, in: Proceedings of the 27th International Conference on International Conference on Machine Learning, Omnipress, Haifa, Israel, 2010, pp. 807—814.